Identification and interpretation of systematic influences caused by changing atmospheric conditions in multitemporal Permanent Laser Scanning

Daniel CZERWONKA-SCHRÖDER[1] (ORCID 0009-0008-0314-5674), Yihui YANG[2] (ORCID 0000-0002-0646-1073) & Christoph HOLST[2] (ORCID 0000-0002-7966-4322)

[1] Department of Geodesy, Bochum University of Applied Sciences,
daniel.czerwonka-schroeder@hs-bochum.de (corresponding author)

[2] Chair of Engineering Geodesy, TUM School of Engineering and Design,
Technical University of Munich

DOI: 10.3217/978-3-99161-070-0-006, CC BY 4.0

1 Introduction and Motivation

Permanent Laser Scanning (PLS) enables the near-continuous acquisition of three-dimensional scenes from a fixed or re-mountable sensor position and has become an established approach for the monitoring of time-dependent changes in engineering and natural environments (LINDENBERGH ET AL., 2025). In contrast to campaign-based terrestrial laser scanning (TLS), PLS produces dense four-dimensional datasets (3D + time), which provide new opportunities for analyzing complex temporal changes of object surfaces, while at the same time imposing fundamentally different requirements on data handling, processing, and interpretation (CZERWONKA-SCHRÖDER, 2023).

A process-oriented view in PLS is required for two main reasons. First, the permanent and high-frequency operation of PLS results in large volumes of point cloud data, which necessitate a structured and consistent measurement and processing concept. Second, the dense temporal sampling inherent to PLS makes systematic influences in the data explicitly visible. PLS is affected by systematic influences, such as atmospheric effects or the movement of the scanner platform, which have been documented in several studies (e.g. FRIEDLI ET AL., 2019; KUSCHNERUS ET AL., 2021; VOORDENDAG ET AL., 2022; SCHRÖDER ET AL., 2022; YANG ET AL., 2025). In campaign-based TLS applications, the same effects are also present, but they are often less apparent or implicitly reduced by selecting favorable measurement epochs, survey configurations or by campaign-wise geo-referencing.

Atmospheric effects and platform motion directly affect the captured point clouds, which serves as the primary data product for subsequent analysis. If such systematic influences are not adequately considered, misinterpretations of multitemporal PLS data are unavoidable. To consistently relate multitemporal epochs within a common reference frame and to account for effects acting approximately homogeneously on the scene, the estimation of interepochal transformation parameters, comprising translations and rotations, is required (KUSCHNERUS ET AL., 2021). A robust, purely data-driven approach for estimating these transformation parameters and for the targetless registration of multitemporal point clouds has been presented by YANG AND HOLST (2025). This provides a reliable methodological basis for

consistently aligning dense PLS data in a common reference frame and simultaneously delivering the optimal transformation parameter time series.

In this contribution, point cloud registration is not solely regarded as a corrective processing step, but as an integral component of the measurement concept in PLS. The transformation parameters estimated during registration are interpreted as observations rather than auxiliary results. Their temporal variability reflects the influence of system-related and environmental effects acting on the measurement setup. By analyzing these parameter time series, dominant systematic influences can be identified and separated. This perspective shifts the role of registration from a purely technical necessity towards a source of information on data quality and system behavior. The paper, therefore, focuses on the interpretation of registration-derived transformation parameters to better understand and assess high-frequency PLS time series.

2 Study Area and Data

The study site is the Trierer Augenscheiner, a rock slope located along the Mosel River at the northern periphery of Trier (Rhineland-Palatinate, Germany). The site is subject to gravitational mass movements and poses a direct hazard to adjacent transport infrastructure. The site represents a real-world scenario for continuous, near-real-time monitoring of unstable rock slopes using PLS. The test site was selected within the framework of the AImon5.0 research project (CZERWONKA-SCHRÖDER ET AL., 2025). On 26 January 2023, a rockfall with an estimated volume of approx. 135 m³ occurred, causing substantial damage to the vineyard below. The event highlights the necessity of 4D data to capture the temporal evolution of rockfall processes.

A permanent monitoring installation was operated from 13 December 2023 to 24 August 2025 as an experimental reference setup for assessing the capability of PLS. The installation was implemented on the opposite side of the river at the municipal swimming pool facilities, resulting in an average sensor-to-object distance of approximately 250–300 m. The core sensor of the system is a RIEGL VZ-2000i terrestrial laser scanner. The scanner operates in an automated mode and acquires one point cloud per hour with an angular resolution of 17 mgon, complemented by an additional scan every six hours with an angular resolution of 6 mgon.

For independent reference observations, a total station measures 22 prisms at an hourly interval. The prisms are detected also by the laser scanner; nevertheless, they are not used to improve the laser scanning data to be independent from those observations. Two inclination sensors monitor the stability of the pillar at a 15-second sampling interval. Environmental parameters are recorded by a weather station. All analyses presented in this study are performed in the scanner's own coordinate system (SOCS). The SOCS is defined as a right-handed coordinate system with the X-axis aligned with the scanner's main ranging direction, which is illustrated in Figure 1 (X-axis (green), Y-axis (red) and Z-axis (blue)). An overview of the study site and sensor configuration is shown in Figure 1. This study analyzes a subset of the PLS time series covering the period from 17 to 27 August 2024.

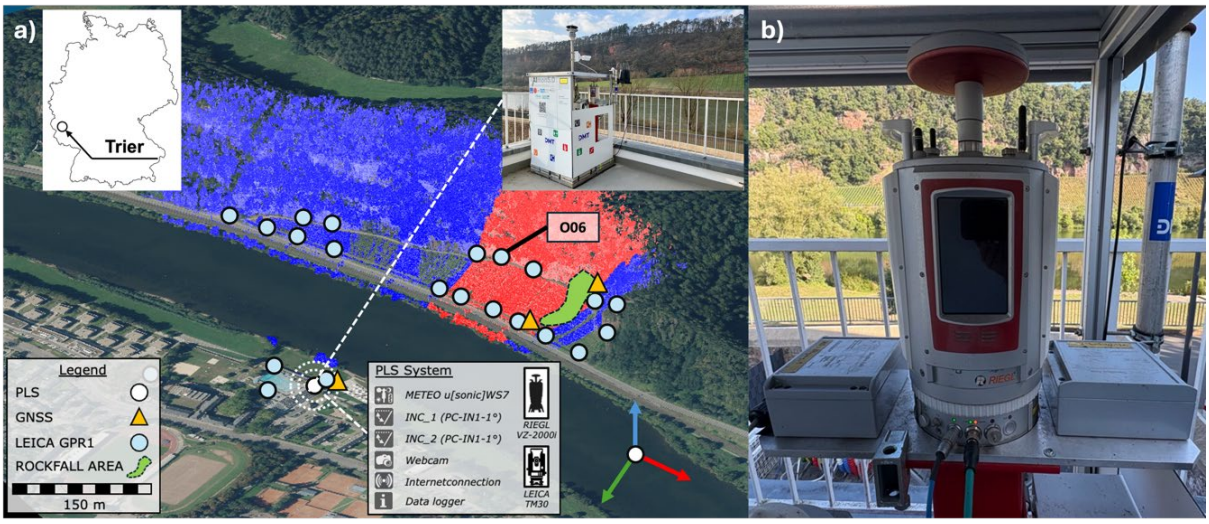

Fig. 1: Overview of the test site at the Trierer Augenscheiner and the monitoring installation. (a) Three-dimensional overview of the test site including the applied sensor technology (background map data: © GeoBasis-DE / LVermGeoRP 2025). (b) Mechanical coupling and inclination sensor installation between the laser scanner and the pillar at the Trier study site.

3 Methodology

This chapter describes the methodological components used to analyze multitemporal PLS data and to account for systematic influences affecting the resulting time series. The applied approach combines several complementary methods, each addressing a specific aspect of the measurement system or its environment, to enable a structured and reproducible investigation of influencing factors.

First, a target-free registration approach is applied to transform all epochs into a common coordinate frame, providing a consistent spatial reference for temporal analysis (Sec. 3.1). Independent geodetic reference observations based on a prism network are then introduced to enable external verification of scanner-based results (Sec. 3.2), complemented by scanner-based prism detection allowing comparative analyses using identical 3D points (Sec. 3.3). To capture orientation changes of the scanner and pillar independently of the point cloud data, inclination sensors are incorporated (Sec. 3.4). Finally, atmospheric effects are considered through external correction based on local meteorological observations to reduce systematic range distortions (Sec. 3.5).

Together, these methodological components form a coherent framework for isolating and analyzing different sources of systematic effects in high-frequency PLS time series.

3.1 Estimation of multitemporal transformation parameters

To register PLS point clouds into a unified frame, a reference epoch should be first selected, and the scans of all other epochs are aligned with the scan in this reference epoch. The typical strategy is to calculate the transformation parameters by using artificial targets (e.g., signalized planar boards and prisms) fixed at stable positions in the scanned areas. However, several

downsides of this target-based registration strategy are evident despite its superiorities of high reliability (YANG AND SCHWIEGER, 2023), such as the limited number and distribution of targets, the necessity to access the monitored areas, and the possible instability of targets' positions due to unexpected interferences. Therefore, registration methods without using artificial targets should be used to simplify data acquisition and reduce measurement costs. To tackle these challenges, an efficient target-free registration scheme for 4D point clouds, called Piecewise-ICP, is adopted (YANG AND HOLST, 2025). This method can accurately register 4D data from the PLS system based on automatically identified stable areas and is thus robust to unexpected changes and deformations during monitoring.

In Piecewise-ICP, point cloud time series are input and organized according to their time information. The 4D data registration is then decomposed into multiple pairwise registrations, where the pair sequence is determined by assessing the approximate overlap ratio for each potential pairing. Assuming minimal movement of the PLS platform during the monitoring period, all scans are regarded as coarsely aligned. Thereby, a fine registration is directly performed for each pair of point clouds using an efficient and robust method based on a patch-based segmentation strategy, yielding transformation parameters including three rotation angles and three translation components for each pairwise registration. By defining a reference epoch (e.g., the first epoch) and applying the pair sequence information, the final transformation of each point cloud to the reference scan can be computed. Further methodological details can be found in YANG AND HOLST (2025).

3.2 Geodetic reference observations using prisms

The total station measurements are employed to establish an independent geodetic reference frame for the methodological evaluation of PLS-derived quantities. The suitability of this reference frame depends on the temporal stability of the observed prism network and is therefore subject to a formal deformation analysis.

A detailed deformation and stability analysis of the total station prism network (LEICA GPR1 points in Fig. 1) at the Trierer Augenscheiner is presented by SCHULTE ET AL. (2025). The analysis is based on a least-squares adjustment of the original observations and applies established congruence and hypothesis testing procedures to identify stable reference points and potential object point displacements. Reference points that do not satisfy the statistical stability criteria are iteratively excluded from the datum definition, resulting in a consistent and statistically validated reference frame.

For the observation period relevant to this study, the results reported by SCHULTE ET AL. (2025) demonstrate that the prisms remain stable within the sensitivity limits of the applied deformation analysis. On this basis, the total station-derived coordinate time series constitute a methodically verified external reference for the subsequent interpretation of PLS-based analyses.

3.3 Scanner-based prism detection

The detection of corner cube prisms within the laser scanning data is a manufacturer-specific functionality. This capability is based on a dedicated measurement and processing concept that

allows reflective prisms to be identified within a scan and subsequently re-measured using adapted scanner settings. The methodological implementation is described in detail by CZERWONKA-SCHRÖDER (2023). The achievable accuracy of scanner-based prism detection was evaluated in a test field with prism distances of approximately 900–1,200 m. The longitudinal component shows an accuracy of 1.3 mm, while the transversal components exhibits an accuracy of 18.0 mm. The resulting prism coordinates are provided as separate coordinate lists in the SOCS and can be directly used for subsequent analyses and visualizations.

3.4 Inclination sensors and mechanical coupling

Inclination sensors are used to record the relative orientation of the laser scanner in all spatial axes during multitemporal data acquisition. Two inclination sensors (Position Control) are mounted at the interface between the PLS and the supporting pillar. The sensors are integrated using a mechanically rigid coupling element designed based on CAD models of the scanner geometry. One sensor is aligned parallel to the X-axis and the second sensor parallel to the Y-axis of the SOCS, allowing rotations about both horizontal axes to be recorded. The sensor mounting and mechanical integration at the Trier study site are shown in Figure 1(b).

The inclination measurements represent relative orientation changes between successive epochs. For the subsequent analysis, the inclination values are incorporated by combining them with the scan data using a rotation matrix, accounting for rotations about the X- and Y-axes of the SOCS. A detailed description of the sensor configuration, mechanical coupling, alignment, and data handling is provided in CZERWONKA-SCHRÖDER (2023).

3.5 Atmospheric data and distance correction

Atmospheric conditions influence the propagation velocity of electromagnetic waves and therefore affect range measurements in laser scanning systems. Variations in air density caused by changes in temperature, pressure, and humidity lead to systematic deviations of measured distances (BRUNNER, 1984). The resulting influence primarily manifests as a scale effect. Effects related to beam deflection are not explicitly considered in this study. In PLS, these effects are expressed as structured temporal patterns in multitemporal point cloud series and can exceed the expected measurement accuracy (CZERWONKA-SCHRÖDER, 2023).

Local atmospheric conditions are recorded by a weather station installed at the scanner site and are used to characterize the atmospheric state for each scan epoch. Based on these measurements, atmospheric effects are accounted for by applying a scale correction derived from the refractive properties of air, following the IAG-recommended formulation (ESCHELBACH, 2009; JOECKEL ET AL., 2008).

The internal atmospheric scale correction of the RIEGL laser scanner is disabled, as the integrated sensor does not represent the atmospheric conditions along the laser beam path. Instead, an external refraction-related scale correction based on meteorological parameters recorded by a weather station installed at the scanner site is applied prior to multitemporal registration to ensure consistent correction of range measurements.

4 Results and Analysis

We analyze the prism observations of the PLS without registration first (Sec. 4.1), before estimating multitemporal transformation parameters based on this data (Sec. 4.2), afterwards applying them to the PLS data (Sec. 4.3). To evaluate those results, we focus on atmospheric refraction effects (Sec. 4.4), the influence of platform inclination (Sec. 4.5) and estimated transitional parameters (Sec. 4.6).

4.1 Prism observations without registration

Figure 2 shows the scanner-based coordinate time series of prism O06 for the analysis period. A data gap is present in the time series between 22 August 2024 at 06:00 and 24 August 2024 at 09:00, caused by a temporary software-related issue affecting only the prism detection. The acquisition of the laser scanning data itself was not interrupted. The prism was selected as a representative example, as comparable temporal patterns are observed consistently for multiple prisms. The total station observations confirm stability during the selected period.

In contrast, the prism coordinates derived from PLS exhibit temporal variations. Despite the scanner being installed on a fixed pillar, the time series does not reflect the stability indicated by the total station. The most pronounced variations occur in the Z-component, where periodic deviations with amplitudes of up to approx. 12 cm are observed. Additional periodic variations with amplitudes of approx. 2–3 cm are present in the Y-component, oriented transverse to the line of sight towards the rock slope. Variations in the X-component remain confined to the millimeter range.

The occurrence of these patterns across multiple prisms indicates that the observed effects are not caused by a prism motion itself. Instead, the unregistered prism observations reveal systematic influences affecting the PLS data, originating either from the scanner setup itself or from effects acting along the laser beam propagation path. These results demonstrate that unregistered PLS data are affected by systematic effects and that a registration-based alignment is required, which is applied in the subsequent analysis.

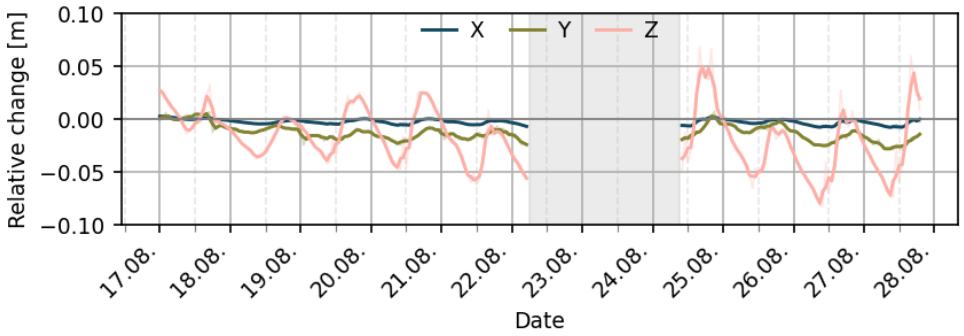

Fig. 2: Scanner-based prism coordinate time series of prism O06 (X, Y, Z) prior to registration for the analysis period from 17 to 27 August 2024.

4.2 Multitemporal transformation parameters

After performing distance correction on the PLS data based on meteorological parameters, 4D point clouds captured during the selected period are all registered to the scan in the reference epoch (August 17th, 00:00) using Piecewise-ICP. Figure 3 shows the identified stable patches utilized for estimating the transformation parameters of one epoch. Most of the stable areas (as highlighted in blue) are located on the surface of nearly vertical rocky cliffs and the vineyard below. These patches ensure that registration remains unaffected by deformed or low-quality areas (such as vegetation regions containing substantial noise). The diversity in patch orientations also enhances the alignment accuracy of the point cloud in all directions.

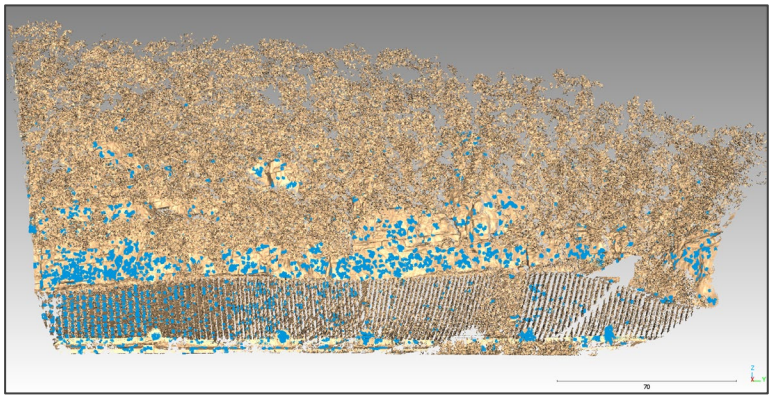

Fig. 3: Identified stable patches by Piecewise-ICP used for registration (blue) in the scanned areas of one monitoring epoch.

The time series of estimated transformation parameters are presented in Figure 4, which exhibits significant variations during the selected period. Specifically, the rotation angles along the Y-axis exhibit a strong diurnal periodicity, varying up to 30 mgon, while the rotation angles around the X- and Z-axes show significantly smaller fluctuations, ranging within ±10 mgon.

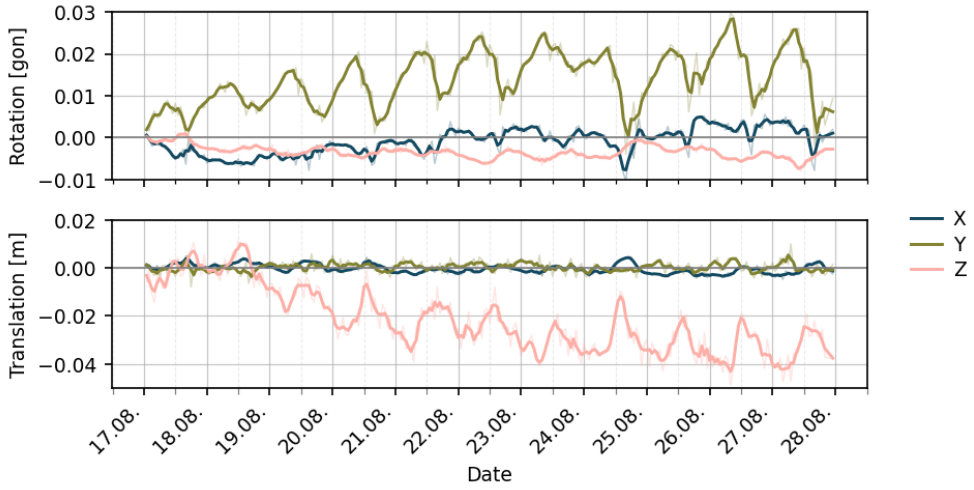

Fig. 4: Time series of estimated transformation parameters for the analysis period.

For the translation, variations in both the X and Y axes are on the order of millimeters and exhibit pronounced randomness. Conversely, the Z-axis translation has undergone significant changes since August 19th, displaying a noticeable periodicity. In particular, Z-axis translation fluctuated within approximately ±1 cm during the first two days. Starting from the third day, it exhibits an overall downward trend, decreasing by 2–3 cm. Furthermore, from the second day onward, the daily variation also increases, with an average amplitude up to 3 cm. Consequently, the maximum Z-axis translation change relative to the reference epoch reached 4–5 cm. A detailed analysis of these phenomena will be provided in Section 4.6.

4.3 Evaluation of the registration by prisms

Figure 5 shows the scanner-based coordinate time series of prism O06 after applying registration-derived transformation parameters. Compared to the unregistered results presented in Section 4.1, the prism coordinates derived from the registered PLS data exhibit a substantially improved temporal behavior.

The most significant change is observed in the Z-component, where the pronounced periodic signal identified prior to registration is effectively minimized and no longer visible. Residual variations remain present, but their magnitude corresponds to the expected accuracy of scanner-based prism detection. Occasional increased amplitudes can still be observed, indicating short-term effects that are neither spatially homogeneous nor temporally persistent and therefore cannot be described by the estimated transformation parameters. The X- and Y-components are also effectively stabilized by registration. While the X-component shows only minor residual variations, the Y-component exhibits slightly increased noise, which can be attributed to the characteristics of the prism detection technique and the measurement geometry. After registration, the scanner-based prism time series are consistent with the confirmed stability by the total station observations, indicating its effective compensation of dominant systematic effects.

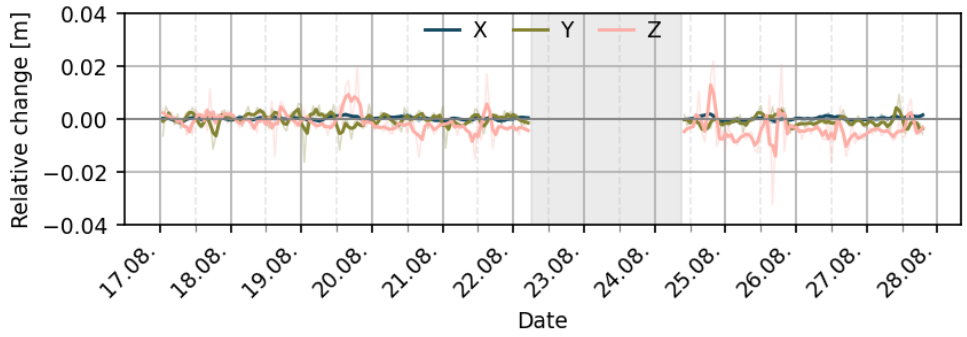

Fig. 5: Scanner-based prism coordinate time series of prism O06 (X, Y, Z) after registration for the analysis period from 17 to 27 August 2024.

4.4 Atmospheric scale effects

Following registration, the transformation parameters are analyzed to identify systematic influencing factors. This section focuses on the effect of distance correction by comparing results with and without external atmospheric correction.

The laser scanner is calibrated for standard laboratory conditions (12 °C, 1000 mbar, 60 % relative humidity). As the internal atmospheric correction was disabled, deviations from these conditions introduce systematic effects that primarily manifest as a scale change of distance measurements.

Figure 6 compares the transformation parameters obtained with and without applying an external atmospheric correction. While the rotation parameters and the translations in Y and Z show only minor and largely random differences, the translation component along the X-axis exhibits higher magnitudes and a pronounced periodic trend. This behavior reflects the acquisition geometry, as the scanner's ranging direction is predominantly aligned with the X-axis and the measured distances of most points are similar in the rockfall areas. Thereby, scale-related effects due to atmospheric effects are primarily absorbed by the X-translation.

The observed differences, amounting to several millimeters in the X-direction, can be attributed to changes in the propagation velocity of the laser signal caused by varying atmospheric conditions. However, compared to the magnitude and temporal structure of the variability observed in Section 4.2, the refraction-related effects are of subordinate importance and do not represent the dominant source of the observed temporal patterns.

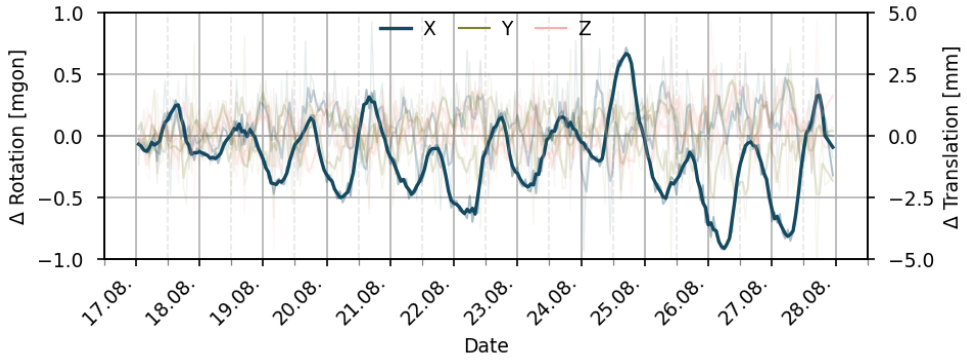

Fig. 6: Difference of estimated transformation parameters before and after atmospheric correction. Rotations (X, Y, Z) and translations in Y and Z show no significant differences and are displayed transparently. A systematic effect is only observed for the X-translation (blue).

4.5 Influence of platform inclination

The pronounced variations in rotation angles along the X and Y axes in Figure 4 indicate that the deviations in PLS data are probably related to the tilt of the scanner platform. To investigate the contribution of the pillar's inclination to estimated transformation parameters, raw PLS data are firstly corrected by the filtered measurements from two inclination sensors as depicted in Section 3.4. The corrected 4D point clouds are then registered to the reference scan by Piecewise-ICP, deriving different transformation parameters as shown in Figure 7.

Overall, the translation values show negligible differences compared to the results without inclination correction, whereas the re-estimated rotation angles exhibit significant changes—particularly the greatly reduced Y-axis rotation angle (compared to Figure 4). This indicates that the tilt of the supporting pillar is the main cause of variations in the horizontal rotation angles estimated by point cloud registration. However, this does not imply that the pillar's tilt

can be fully captured by the registration parameters, as noticeable diurnal angular variations can still be observed from the re-estimated rotation angles in Figure 7. Specifically, the rotation along the X-axis exhibits greater variation after inclination-based correction. This may be attributed to the inclination data in this direction over-compensating for the pillar's tilt, which is ultimately corrected through registration. Meanwhile, the residual Y-axis rotation may arise from three sources: 1) under-compensation of inclination data; 2) systematic laser beam deflection caused by atmospheric refraction; 3) partial absorption of the Y-axis rotation angle by the Z-axis translation parameter. Alternatively, it could result from the combined effects. The role and contribution of these factors require further investigation.

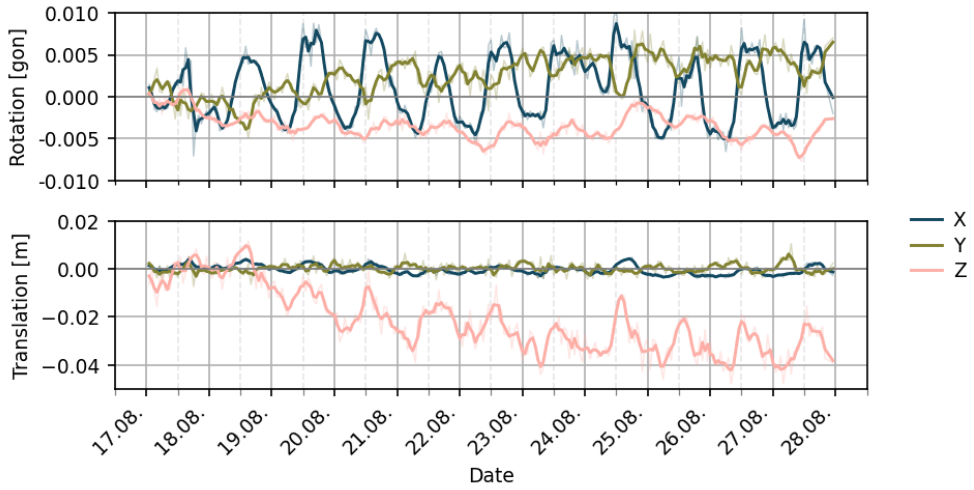

Fig. 7: Time series of estimated transformation parameters after inclination correction for the analysis period.

4.6 Analysis of estimated Z-translations

As observed in both Figure 4 and Figure 7, significant Z-translations in the transformation parameters show variations up to 4 cm with a strong daily periodicity, though the estimated translations along the X and Y axes are minimal and random. The first possible explanations are the height changes of the monitoring platform or the bending effect of atmospheric refraction on the laser beams. However, based on the analysis of total station measurements, both of these effects are very minor, with variations of at most a few millimeters.

To further analyze the impact of different error sources, Figure 8 shows the scanner-based coordinate time series of prism O06 after applying the inclination-based correction. While the residual X-component shows minimal variations owing to the atmospheric distance correction, the Y- and Z-components still exhibit noticeable changes. The observed periodicity in Y-component can be explained by the diurnal rotational behavior of the pillar around the Z-axis. This Z-rotation cannot be captured by the inclination sensors and consequently remains after applying the inclination correction. However, this can be effectively compensated through the adopted registration approach, which explicitly estimates Z-rotations (rf. Figure 4). Although the remaining Z-components (within 2 cm) after inclination correction are slightly larger than those after applying registration (rf. Figure 5), they are significantly reduced by 2–6 cm

compared to those without registration or inclination correction (rf. Figure 2). This indicates that the dominant error source causing vertical shifts in PLS data is the tilt of the pillar. The residual Z-components may result from incomplete tilt correction and/or atmospheric refraction. Further causes will be investigated in future work.

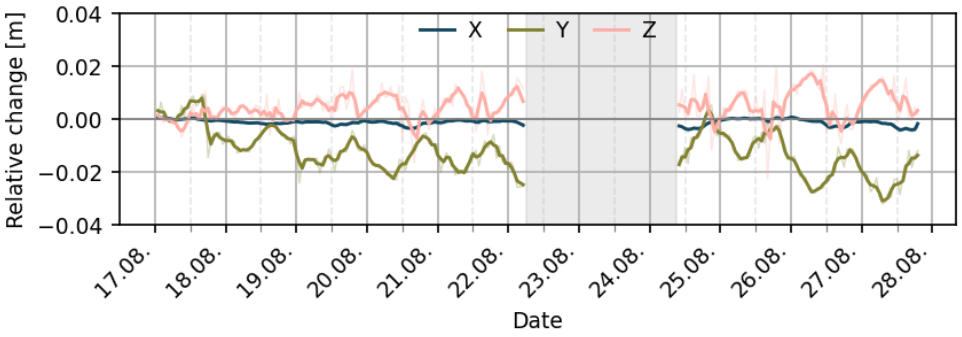

Fig. 8: Scanner-based prism coordinate time series of prism O06 (X, Y, Z) corrected by inclination sensors for the analysis period from 17 to 27 August 2024.

Upon observing the strong correlation between the Z-translation and Y-rotation in the estimated registration parameters (see Figure 4 and Figure 7) and considering that the primary error source originates from the rotational behaviors of the pillar, we attribute the significant Z-translation primarily to the residuals of estimated rotation angles. To verify this assumption, we calculate the vertical translations derived from the measured distance (approx. 320 m) and the differences in Y-axis rotations measured by the inclinometer (blue) and those estimated by registration (green), as demonstrated in Figure 9.

The Z-translations obtained from these two methods are nearly identical, indicating that the Z-translations estimated based on registration are mainly used to compensate for an incomplete estimate of Y-axis rotations to achieve optimal point cloud alignment. Other error sources like atmospheric refraction or instrument-related instability may play a minor role in the estimation of Z-translations.

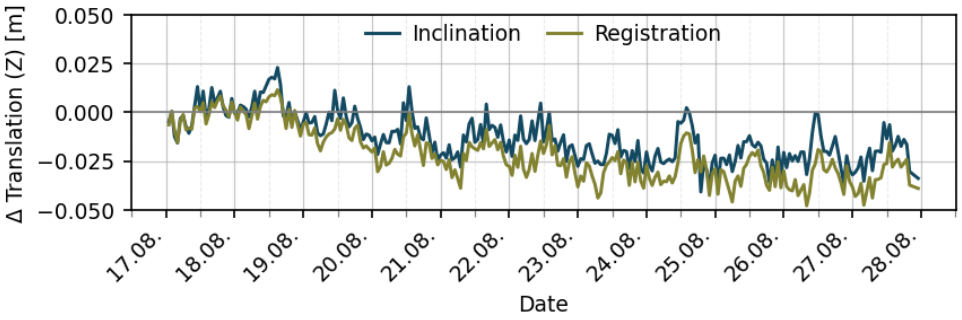

Fig. 9: Difference between the Z-translations from estimated parameters by registration and from the offsets between inclination angles and Y-rotation estimated by registration.

5 Conclusion and Outlook

This contribution demonstrates how point cloud registration parameters and multi-sensor data can be utilized to comprehensively analyze systematic errors in PLS point cloud, taking the PLS data from the Trierer Augenscheiner as an example. The results further confirm that the Piecewise-ICP provides a reliable and precise method for the registration of multitemporal PLS point clouds and can be effectively integrated into continuous monitoring workflows.

First, the Piecewise-ICP algorithm is applied to accurately register the 4D PLS point cloud after distance correction and to derive time series of transformation parameters. These parameters are not only used for data correction, but also serve as an integral part of the PLS measurement concept. They reveal pronounced systematic errors in the point clouds with a clear diurnal periodicity. By identifying stable prism center coordinates, the registration method is validated and shown to significantly reduce systematic errors in the PLS data. A comparison with inclination-based corrections indicates that the dominant systematical errors originate from platform tilts. Both registration-based and inclination-based corrections effectively mitigate pillar's rotation-induced systematic errors. However, torsion around the vertical axis remains uncompensated by limited inclination data, whereas registration can successfully extract pillar's rotation around this direction and further reduce the residual errors. In addition, a mutual compensation effect between rotation angles and translation components is observed in the registration parameters. This indicates that, in certain cases, the estimated transformation parameters may not fully represent the true physical quantities causing point cloud rotation or translation. Nevertheless, the registration-based approach can account for multiple error sources and effectively reduce resulting deviations.

Overall, the analytical methods and result interpretations presented in this study provide valuable insights for understanding and analyzing the composition of PLS systematic error sources and their respective contributions. At the same time, the presented interpretations should be understood as site- and setup-specific. While this study identifies relevant influencing factors and illustrates their impact on PLS data, systematic effects must always be evaluated individually with respect to the specific measurement configuration and environmental conditions. As the mathematical registration model is not directly coupled to the underlying physical processes, different monitoring sites may exhibit different dominant effects and parameter interactions.

Future work will focus on analyzing data from extended time periods and on developing quantitative models to describe atmospheric refraction effects on laser beam bending.

References

BRUNNER, F. K. (1984). Overview of Geodetic Refraction Studies. In F. K. Brunner (Ed.), Geodetic Refraction - Effects of Electromagnetic Wave Propagation Through the Atmosphere (p. 1–6). Springer.

CZERWONKA-SCHRÖDER, D. (2023). Konzeption einer qualitätsgesicherten Implementierung eines Echtzeitassistenzsystems basierend auf einem terrestrischen Long Range Laserscanner, Reihe C

(913), Deutsche Geodätische Kommission bei der Bayerischen Akademie der Wissenschaften. Phd thesis.

CZERWONKA-SCHRÖDER, D., SCHULTE, F., ALBERT, J., HÖFLE, B., HOLST, C., & ZIMMERMANN, K. (2025). AImon5.0 – Real-time monitoring of gravitational mass movements and critical infrastructure risk management with AI-assisted 3D metrology. In Proc. of the 6th Joint International Symposium on Deformation Monitoring (JISDM), Karlsruhe.

ESCHELBACH, C. (2009). Refraktionskorrekturbestimmung durch Modellierung des Impuls-und Wärmeflusses in der Rauhigkeitsschicht, Schriftenreihe des Studiengangs Geodäsie und Geoinformatik (2009,1), University of Karlsruhe (TH). Phd thesis.

FRIEDLI, E., PRESL, R., & WIESER, A. (2019). Influence of atmospheric refraction on terrestrial laser scanning at long range. In Proc. of the 4th Joint International Symposium on Deformation Monitoring (JISDM), Athens.

KUSCHNERUS, M., SCHRÖDER, D., AND LINDENBERGH, R. (2021). Environmental influences on the stability of a permanently installed laser scanner. International Archives of the Photogrammetry, Remote Sensing and Spatial Information Sciences, 43(B2-2021).

LINDENBERGH, R., ANDERS, K., CAMPOS, M., CZERWONKA-SCHRÖDER, D., HÖFLE, B., KUSCHNERUS, M., PUTTONEN, E., PRINZ, R., RUTZINGER, M., VOORDENDAG, A., & VOS, S. (2025). Permanent terrestrial laser scanning for near-continuous environmental observations: Systems, methods, challenges and applications. ISPRS Open Journal of Photogrammetry and Remote Sensing, 17, 100094.

JOECKEL, R., STOBER, M., & HUEP, W. (2008). Elektronische Entfernungs- und Richtungsmessung und ihre Integration in aktuelle Positionierungsverfahren. Wichmann.

SCHRÖDER, D., ANDERS, K., WINIWARTER, L. & WUJANZ, D. (2022). Permanent terrestrial LiDAR monitoring in mining, natural hazard prevention and infrastructure protection – Chances, risks, and challenges: A case study of a rockfall in Tyrol, Austria. In Proc. of the 5th Joint International Symposium on Deformation Monitoring (JISDM), Valencia.

SCHULTE, F., SCHNEIDER, L., LÖSLER, M., PRINTZ, S. & CZERWONKA-SCHRÖDER, D. (2025). Automatic geodetic monitoring with total stations based on the open source software library JAG3D - Case study of a rockfall in Trier/Germany. In Proc. of the 6th Joint International Symposium on Deformation Monitoring (JISDM), Karlsruhe.

VOORDENDAG, A. B., GOGER, B., KLUG, C., PRINZ, R., RUTZINGER, M., & KASER, G. (2022). The stability of a permanent terrestrial laser scanning system - a case study with hourly scans. The International Archives of the Photogrammetry, Remote Sensing and Spatial Information Sciences, XLIII-B2-2022:1093–1099.

YANG, Y., CZERWONKA-SCHRÖDER, D., SEUFERT, P., & HOLST, C. (2025). Using point cloud registration to mitigate systematic errors in permanent laser scanning-based landslide monitoring. In Proc. of the 6th Joint International Symposium on Deformation Monitoring (JISDM), Karlsruhe.

YANG, Y., AND HOLST, C. (2025). Piecewise-ICP: Efficient and robust registration for 4D point clouds in permanent laser scanning. ISPRS Journal of Photogrammetry and Remote Sensing, 227, 481–500.

YANG, Y., AND SCHWIEGER, V. (2023). Supervoxel-based targetless registration and identification of stable areas for deformed point clouds. Journal of Applied Geodesy, 17(2), 161–170.